ORGANOMETALLICS

pubs.acs.org/Organometallics Article

Catalytic Deuteration of $C(sp^2)$ —H Bonds of Substituted (Hetero)arenes in a Pt(II) CNN-Pincer Complex/2,2,2-Trifluoroethanol- d_1 System: Effect of Substituents on the Reaction Rate and Selectivity

Morgan Kramer, David Watts, and Andrei N. Vedernikov*



Cite This: Organometallics 2020, 39, 4102-4114



ACCESS

Metrics & More

Article Recommendations

Supporting Information

ABSTRACT: Thirty four (hetero)arene derivatives have been tested in catalytic H/D exchange reactions involving their $C(sp^2)$ —H bonds and 2,2,2-trifluoroethanol- d_1 (TFE- d_1) in the presence of the homogeneous Pt(II) complex 1 supported by a sulfonated CNN-pincer ligand at 80 °C. The 18 substrates, including one pharmaceutical (naproxen), that are stable in the presence of 1 and are active in the H/D exchange reaction have been characterized by their position-specific extent of deuteration and, in a number of cases, the reaction kinetic selectivity. For the most reactive substrates the extent of deuteration approaches the expected statistical distribution of the exchangeable H and D atoms: e.g., 67–69% for phenol after 23 h and 88% for indole β-CH bonds after 45 min. For a few substrates (N_i N-dimethylaniline, indole,

Exclusively C(sp²)-H bond - selective

0.1-0.5 mol% 1

$$x$$
 TFE-OD

 80 °C

 x TFE-OD

 x Naproxen- x Naproxen- x Naproxen- x Naproxen- x Naproxen

nitrobenzene) the H/D exchange is highly position selective. No satisfactory correlation was found between the position-specific (meta, para) H/D exchange rate constants for X-monosubstituted benzenes and Hammett σ_X constants. This observation was proposed to be related to the concerted nature of the CH bond activation, the rate-determining CH bond oxidative addition at a Pt(II) center. A novel scale of Hammett σ_X^M constants was introduced to characterize the reactivity of $C(sp^2)$ -H bonds in transition-metal-mediated reactions. The experimentally determined position-specific Gibbs energies of activation of the H/D exchange in substituted benzenes (meta and para positions) as well as in thiophene (α and β positions) were matched satisfactorily using DFT calculations.

1. INTRODUCTION

Since the discovery of the first homogeneous platinum(II) complexes capable of hydrocarbon C–H bond activation observed initially as an H/D exchange between hydrocarbon substrates and $CD_3CO_2D-D_2O_7^{1,2}$ catalytic H/D exchange experiments have become a prime and simple tool to probe the reactivity of various transition-metal species toward C–H bonds. On the practical side, various homogeneous transition-metal complexes are now used as catalysts in H/D exchange reactions.³ Recently, we have reported the preparation of Pt(II) complexes 1–3 supported by our novel CNN-pincer ligands (Chart 1) that appeared to be some of the most active platinum-based homogeneous catalysts for H/D exchange between $C(sp^2)$ –H bonds of arenes (H_nSub) and 2,2,2-trifluoroethanol- d_1 (TFE) (eq 1),^{4,5} in comparison to other reported Pt-based systems:^{6,7}

$$H_nSub + nCF_3CH_2OD \rightarrow D_nSub + nCF_3CH_2OH$$
 (1)

For instance, reaction 1 with 10 vol %benzene as a substrate and complex 1 as a catalyst can be observed at 20 $^{\circ}$ C; the

Chart 1. Pt(II) Aqua Complexes 1-3 Supported by Sulfonated CNN-Pincer Ligands

$$SO_3$$
 O_3S O_3S O_3S O_3S O_3S O_3S O_4S O_4S

catalyst's turnover frequency reaches 46 h⁻¹ at 80 °C.⁴ Our subsequent study of reactivity of complex 1 led us to the discovery of Pt-mediated stoichiometric CH oxidation with O_2

Received: September 28, 2020 Published: November 10, 2020





Chart 2. Aromatic Substrates H_n Sub Studied in This Work and the Extent of Their Deuterium Incorporation, x, Observed after the Time Indicated Using ~ 1 M Solutions of the Substrates in Wet TFE- d_1 with Complex 1 as a Catalyst at 80 °C^a

^aThe values in parentheses show the extent of deuteration x observed in the absence of catalyst 1 after otherwise identical conditions.

of various arenes ArH and complex 1 (eq 2). The reaction produces arene-derived Pt(IV) aryl hydroxo complexes LPt^{IV}Ar(OH) and can involve both electron-rich o- and m-dialkylbenzenes ArH (alkyl = Me, t-Bu), as well as electron-poor o-dichloro- and o-difluorobenzenes. Interestingly, except for o-F₂C₆H₄, these oxidation reactions result in >90% selective formation of a single isomer of the derived LPt^{IV}Ar(OH) compounds. ⁸

According to our kinetics study of reaction 2, the arene CH activation at a Pt(II) center may be responsible for the selectivity of oxidation of the benzene derivatives above. Hence, a better understanding of the reactivity of complex 1 in reaction 1 with respect to various arene $C(sp^2)$ —H bonds, as well as the effect of arene substitution on such reactivity, may be important for future development of Pt-mediated CH functionalization chemistry. When complexes 2 and 3 are considered as the catalysts of the H/D exchange reaction (eq 1), it is worth mentioning that they are more reactive than 1 but they also lose their activity much more rapidly at 80 °C (complex 2) or already above 20 °C (complex 3)⁵ due to the formation of poorly soluble polynuclear platinum species. Hence, in this work we focus on the H/D exchange reaction

(1) catalyzed by complex 1. We use a wide range of arenes bearing various electron-donating and electron-withdrawing functional groups, as well as some heteroarenes, 4-32 (Charts 1-3). By using ¹H NMR spectroscopy and measuring the initial reaction 1 rate, we were able to determine the reaction kinetic selectivity involving specific types of C(sp²)-H bonds producing well-resolved ¹H NMR signals. Knowledge of the kinetic (regio)selectivity of the transition-metal complexes with respect to various arene C(sp²)-H bonds^{2,6,7,9-12} is limited, especially for Pt-based systems. 2,6,7 We use the rates of H/D exchange at the meta and para positions of monosubstituted benzene derivatives in Chart 2 to introduce a new scale of Hammett constants, $\sigma_{\rm X}^{\ \ M}$, for metal-assisted C–H bond activation reactions. An additional result of this study of the reactivity of a wide range of substrates in Charts 2-4 is the information about the functional group tolerance of complex 1. Notably, we also tested the performance of catalyst 1 in the deuteration of two pharmaceuticals, ibuprofen (33) and naproxen (34) (Chart 4), thus probing the possible application of Pt-catalyzed H/D exchange for deuterium labeling of medicinal compounds. A detailed report of these studies is provided below.

2. RESULTS AND DISCUSSION

2.1. Experimental Setup and Expected Extent of Substrate Deuteration. The catalytic H/D exchange between aromatic substrates H_n Sub and TFE- d_1 (eq 1) used

Chart 3. Aromatic Substrates H_n Sub That Either Engage in Side Reactions under the Conditions Indicated in Chart 2 or Are Inactive in the H/D Exchange

Substrates that engage in side reactions

Inert substrates

$$CF_3$$
 SO_2NH_2 CC_2

Substrates demonstrating strong coordination to 1

Chart 4. Pharmaceuticals 33 and 34 Probed in the H/D Exchange Experiments

as a deuterium source was carried out at 80 °C using, typically, 0.1-0.5 mol % of complex 1 as a catalyst. 4,5 In a typical experiment 0.050 mL of H_nSub (or ~50 mg for solids) was dissolved in 0.450 mL of wet TFE-d₁ containing 0.150 M D₂O and $6-12 \mu \text{mol}$ of catalyst 1. The water additive was shown earlier to slow down the catalyst deactivation caused by the formation of poorly soluble polynuclear species.⁴ The reactions were monitored by ¹H NMR spectroscopy using the TFE-d₁ CH₂ group signal as an internal reference. To estimate the initial reaction rate, the conversion of substrates was checked more often in the period of time corresponding to no more than ~10% substrate conversion and minimal catalyst deactivation.4 Most of the substrates were used with a concentration of ~ 1 M, which corresponds to an $\sim 1-6$ M concentration of the arene $C(sp^2)$ -H bonds of a specific type. In none of our experiments were we able to observe H/D exchange involving C(sp³)-H bonds of alkyl groups. The total concentration of exchangeable deuterium from TFE- d_1 is ~12.5 M, which translates to the expected extent of the substrate's deuteration of ~68-81% upon reaching a hypothetical statistical distribution of deuterium between solvent and all reactive CH bonds of the substrate. In fact, a ≥67% deuteration was observed for the three most reactive

compounds, phenol (9), N,N-dimethylaniline (10), and β -CH bonds of indole (17), by the end of their respective reaction periods (Chart 2). Not all of the compounds 5-34 tested in this work were deuterated under these conditions. The substrates active in the H/D exchange (1) are included in Chart 2 and, in part, Chart 4 (naproxen 34). On the other end of the reactivity series are the substrates shown in Chart 3, as well as ibuprofen (33) (Chart 4). These compounds engage in more or less rapid side reactions or decompose in the presence of 1 (pyrrole (18), furan (19), iodobenzene (20), styrene (21), and phenylacetylene (22)), do not change in the presence of 1 (trifluoromethylbenzene (23), benzenesulfonamide (24), o-dichlorobenzene (25), and ibuprofen (33)), or are able to strongly coordinate to a Pt(II) center in complex 1 thus effectively inhibiting the H/D exchange (e.g., benzonitrile, pyridine, pyrimidine, and pyrazole, 26–32). In practical terms, for substrates 23-33 the extent of deuteration did not exceed ~2%.

Notably, the use of CD_3CO_2D as a solvent and a source of exchangeable deuterium was also attempted and resulted in slower reaction rates. For example, the extent of deuteration of benzene in CD_3CO_2D solution was 14% after 26 h, noticeably lower than 40% with TFE- d_1 after 22 h (Chart 2).

2.2. Stability of Catalyst 1. Background H/D Exchange Reactivity with TFE- d_1 . The potential issues that may affect our ability to estimate the reactivity of 1 in reaction 1 with respect to a specific substrate's CH bonds may be a strong coordination of a substrate to 1, the catalyst decomposition under our reaction conditions, and a background H/D exchange.

Not all Pt(II)-coordinating substrates may be unreactive in H/D exchange. In particular, N,N-dimethylaniline forms an adduct with complex 1, but according to our observations (Chart 2), this substrate is very active in reaction 1, thus suggesting that the adduct with 1 is weak. In particular, the dark purple platinum complex 35 could be isolated from a solution of 1 in a 1/1 (v/v) mixture of N₁N-dimethylaniline and TFE upon precipitation with diethyl ether. The resulting solid is stable under an argon atmosphere and in methanol-d₄ solution for at least 72 h, according to ¹H NMR spectroscopy. In the ¹H NMR spectrum of the solution two N-CH₃ group signals of equal intensity are observed, along with signals of a Pt-coordinated CNN-pincer ligand of matching intensity, thus suggesting the formation of the adduct LPt(PhNMe₂) (35). The adduct coexists in an apparent equilibrium with an approximately equimolar amount of free PhNMe2 and, presumably, a methanol analogue of 1, LPt(MeOH), thus suggesting that the stability of the adduct 35 is low. Similarly, the formation of an adduct between complex 1 and thiophene was detected by ¹H NMR but our attempts to isolate the adduct were not successful because of its even lower stability. Thiophene is also very active in the H/D exchange (reaction

A catalyst deactivation due to the formation of a light yellow precipitate that was not identified was observed for benzoic acid after about 6 h of reaction. Accordingly, the H/D exchange reactivity of this substrate was only analyzed for the first 6 h. For a few other substrates such as chloro- and bromobenzene formation of a red precipitate, presumably the dinuclear product of the decomposition of catalyst 1 decomposition, 4,5 was observed, but only by the end of the monitored reaction 1 period (~24 h). Oxidative addition of the bromobenzene C-Br bond at a Pt(II) center may also be involved to some extent.

To get a better estimate of the reactivity of catalyst 1, in addition to considering the catalyst deactivation, the H/D exchange of all studied substrates in reaction 1 was analyzed in the absence of 1 (Scheme 1a), as well as in the presence of 1

Scheme 1. Background and Pt-Catalyzed H/D Exchange between a Substrate H_"Sub and TFE-d₁

$$H_nSub + nCF_3CH_2OD \xrightarrow{k_b} D_nSub + nCF_3CH_2OH$$
 (a)

$$H_nSub + nCF_3CH_2OD = D_nSub + nCF_3CH_2OH$$
 (b)

(Scheme 1b). The contribution of the background reaction to the deuteration of substrate C-H bonds was considered for the initial reaction period (<10% deuteration) and by the end of our experiments (typically, \sim 24 h); the latter contribution is indicated in parentheses in Chart 2.

In fact, the background reaction contribution to the initial rate of reaction 1 was not detected for any of the substrates in Chart 2. The background reaction for *N*,*N*-dimethylaniline was

only noticeable after 24 h (Chart 2, in parentheses). For indole the background reaction was not noticeable until after ~90 min. The reaction (1) of indole catalyzed by 1 is very fast with 3.6% catalyst loading, and a close to statistical 88% extent of deuteration of indole β -CH bonds is reached after 45 min of reaction, well before the background reaction becomes detectable.

For the rest of the substrates in Chart 2 no noticeable H/D exchange was observed in the absence of the catalyst 1 and no visible sign of the catalyst decomposition was detected. The reactivity and selectivity of catalytic deuteration of substrates shown in Chart 2 are discussed next.

2.3. Reaction 1 Kinetics Model and Initial Rates of CH Activation. The reaction 1 mechanism with benzene as a substrate was studied earlier by means of kinetics, mechanistic tests, the DFT calculations.^{4,5} It was found that the initial rate of the reaction in Scheme 1b is first order in both the substrate CH bond concentration, [C-H], and the catalyst 1 concentration, [1], (eq 3):

$$\frac{d[C-D]}{dt} = k_c[C-H][1] \quad \text{initial rates}$$
(3)

The proposed reaction sequence responsible for the substrate/ TFE- d_1 H/D exchange, slightly modified in comparison to the original proposal,⁴ is presented in Scheme 2. It involves an arene coordination step a to form the σ -arene complex $^{\text{CNN}}\mathbf{1}_{\text{ArX}}$ with a CNN-coordinated pincer ligand, an isomerization step bto form an isomer CNO 1 with a CNO-coordinated pincer ligand, a rate-limiting CH bond oxidative addition to a Pt(II) center at step c, via the transition state TS_{Ar-X} , and a redox isomerization of the resulting Pt(IV) hydrido complex $1_{(Ar)(X)}$ at step d via the lower-energy transition state TS_3 (Scheme 2) to form the Pt(II) aryl 1- X_{Ar} and a facile H/D exchange of the latter with TFE- d_1 or D_2O . The possible involvement of the Pt(II) aryl 1- X_{Ar} and its formation via TS_3 was not considered in the earlier model.⁴ The details of the DFT calculations carried out in this work are given in section 2.5 and in the Supporting Information.

For the purpose of subsequent discussion we assume that the same rate law (3) and the same general mechanism are valid for other substrates in Chart 2. We will use the effective catalytic rate constants k_c for each specific type of a substrate's $C(sp^2)$ -H bond as a measure of the C-H bond reactivity toward catalyst 1. The k_c values are calculated using eq 4:

$$k_{\rm c} = \frac{\rm d[C-D]}{\rm d} \frac{1}{\rm [C-H]} \frac{1}{\rm [1]} \quad \text{initial rates} \tag{4}$$

In turn, the initial rate of incorporation of deuterium into a substrate, $\frac{d[C-D]}{dt}$, is determined using the least-squares fitting procedure during the reaction period corresponding to the substrate's conversion not exceeding 10% (see Figure 1 for an example of initial rate calculations for anisole).

In our experiments involving some monosubstituted benzene derivatives only their m-C(sp²)-H bond 1 H NMR signals were resolved well enough to allow for an accurate integration. Accordingly, the corresponding initial rates and rate constants for their m-C(sp²)-H bonds, $k_{c,m}$, were calculated (Figure 1, right). In turn, the signals produced by o- and p-CH bonds of these substrates were integrated together, thus allowing the calculation of the average reaction rates and the average rate constants, $k_{c,o-p}$, for these C(sp²)-H bonds (Figure 1, left).

Scheme 2. Proposed Reaction Sequence Involved in the H/D Exchange between Arene $C(sp^2)$ -H bonds and TFE- d_1 Catalyzed by Complex 1^a

^aThe standard Gibbs energies for individual reaction steps for TFE solutions at 298 K (blue type) are given for benzene (C_6H_6) in kcal/mol. ⁴

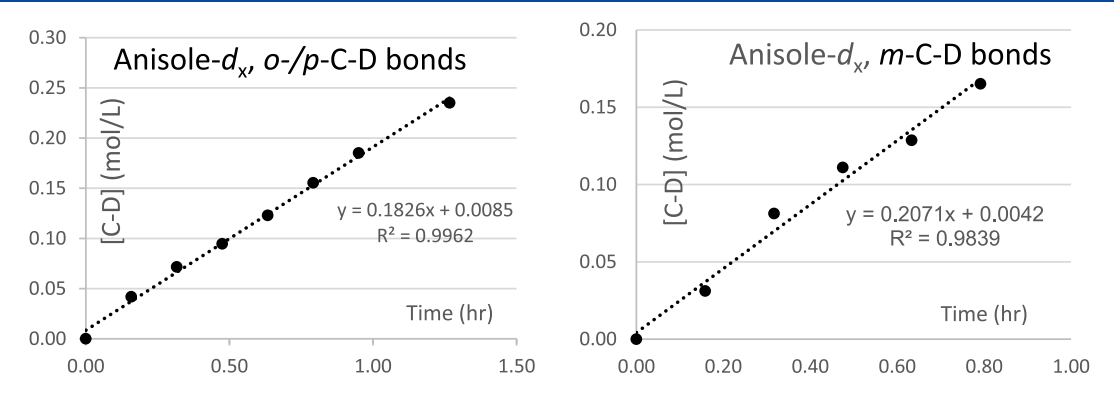


Figure 1. Concentration of $C(sp^2)$ -D bonds of anisole- d_x resulting from reaction 1 between anisole and TFE- d_1 catalyzed by complex 1, as a function of time in the reaction's initial period at 80 °C: a plot for the anisole- d_x o- and p-CD bonds (left) and a plot for the product m-CD bonds (right). The initial concentrations $[C_6H_5OCH_3]_0 = 0.87$ M and [1] = 0.0138 M, and the resulting rate constants are $k_{c,o-p} = 5.1 \pm 0.1$ M⁻¹ h⁻¹ and $k_{c,m} = 8.6 \pm 0.5$ M⁻¹ h⁻¹.

Finally, for substrates containing more than one type of arene $C(\operatorname{sp}^2)$ —H bond a weighted average value, $k_{\operatorname{c-all}}$, were also calculated. These values can be used for the most general comparison of substrate reactivity. The resulting average values, $k_{\operatorname{c-all}}$, and the individual CH bond k_{c} values are given in Table 1. The k_{c} value for $C_{\operatorname{6}}H_{\operatorname{6}}$ will be used as a reference in the following discussion.

2.4. Reactivity of Benzene Derivatives 5-15. The first two substrates, p-xylene (5) and mesitylene (6), that follow benzene in Table 1 contain one or two methyl substituents in the position *ortho* to the substrate $C(sp^2)$ -H bonds. The methyl groups make these substrates electron-richer, in comparison to benzene. Notably, in the transition states TS_{Ar-X} corresponding to oxidative addition of an o-CH bond to a Pt(II) center a noticeable steric interference is anticipated between these substrates' methyl substituents and the Ptcoordinated oxygen atom of the pincer ligand of the catalyst 1, as shown in Figure 2. These steric interactions destabilize the transition states. Overall, the k_c values for benzene (4), pxylene (5), and mesitylene (6) (Table 1) decrease in the sequence benzene > p-xylene ≫ mesitylene, but it is not clear if the electronic effects of the methyl groups work in the same or in the opposite direction, in comparison to the steric interactions in the transition state. The subsequent analysis of reactivity of monosubstituted benzene derivatives suggests that the steric and electronic effects change in the opposite directions (*vide infra*).

To be able to exclude the substituents' steric effect from consideration as the factor affecting the reactivity of monosubstituted benzene derivatives in Chart 2, and focus on the substituents' purely electronic effects, we will consider reactions involving these substrates' *m*- and *p*-CH bonds.

When considering m- and p-CH bonds of monosubstituted benzene derivatives 7, 9-12, 14, and 15, first, we wanted to see if there is a satisfactory correlation between the Gibbs energies of activation of reaction 1 involving these bonds and a simple substituent parameter such as the corresponding Hammett $\sigma_{\rm X}$ constant.¹³ A plot of the experimentally found reaction Gibbs energies of activation, $\Delta G_{353}^{\dagger}(\exp)$, vs the substituent σ_X values is given in Figure 3. The plot shows the absence of any good correlation. Still, one can notice that, overall, reaction 1 tends to be slower for substrates with electron-withdrawing groups, NO2, CO2H, and halogens F and Cl (see also $\sigma_{\text{c-all}}$ values for these substrates and bromobenzene (13) in Table 1), in comparison to benzene. In turn, the rate constants for the H/D exchange involving m-CH bonds of phenol (9) and anisole (7) are slightly larger than those for benzene and the substrates bearing MeO and OH groups.

Table 1. Reaction 1 Rate Constants k_c (Eq 3) and the Corresponding Gibbs Energies of Activation for the H/D Exchange between Specific C(sp²)-H Bonds of Substrates 4-16 and TFE- d_1 catalyzed by 1 at 80 °C^a

		$k_{\sigma}^{b} \mathrm{M}^{-1} \mathrm{h}^{-1}$	Gibbs energy of activation, kcal/mol				
substrate	CH bond		$\Delta G_{353}^{\dagger}(\exp)$, experiment	$\Delta G_{298}^{\dagger} (\mathrm{DFT/gas\ phase})$	$\Delta G_{298}^{\dagger} (\mathrm{DFT/TFE})$		
benzene (4)	all	6.8 ± 0.4	25.2 ± 0.1	22.5	22.3		
p-xylene (51)	all $C(sp^2)$ -H	3.7 ± 0.4	25.6 ± 0.1	27.5	27.0		
mesitylene (6)	all C(sp ²)-H	0.52 ± 0.02					
anisole (7)	о-СН, р-СН	5.1 ± 0.1^{c}					
	m-CH	8.6 ± 0.5	25.0 ± 0.1	22.8	n/a^d		
	all	6.5 ± 0.3^{e}					
benzodioxole (8)	all C(sp ²)-H	6.5 ± 0.9^{e}					
phenol (9)	о-СН, р-СН	4.9 ± 0.7^{c}					
	m-CH	7.3 ± 0.4	25.1 ± 0.1	23.1	23.5		
	all	5.9 ± 0.6^{e}					
N,N-dimethylaniline (10)	о-СН, р-СН	21 ± 1^c					
	m-CH	3.1 ± 0.3	25.7 ± 0.1	22.4	n/a^d		
	all C(sp ²)-H	14.0 ± 0.9^{e}					
fluorobenzene (11)	o-CH	0.70 ± 0.12	26.8 ± 0.1	24.6	23.6		
	p-CH	1.3 ± 0.22	26.3 ± 0.1	24.0	23.9		
	m-CH	1.43 ± 0.06	26.3 ± 0.1	24.2	24.4		
	all	1.1 ± 0.27^{e}					
chlorobenzene (12)	o-CH	2.2 ± 0.3	26.0 ± 0.1	29.4	28.8		
	p-CH	2.7 ± 0.8	25.8 ± 0.2	23.6	23.9		
	m-CH	3.2 ± 0.2	25.7 ± 0.1	23.6	24.0		
	all	2.7 ± 0.1^{e}					
bromobenzene (13)	all	2.4 ± 0.2^{e}					
nitrobenzene (14)	o-CH	0.00					
	p-CH	0.9 ± 0.3	26.6 ± 0.2	25.2	25.1		
	m-CH	0.35 ± 0.06	27.3 ± 0.1	24.8	25.2		
	all	0.33 ± 0.04^{e}					
benzoic acid (15)	о-СН, р-СН	0.78 ± 0.06					
	m-CH	2.5 ± 0.8	25.9 ± 0.2	24.4	n/a^d		
	all	1.5 ± 0.4^{e}					
thiophene (16)	α -CH	18 ± 1	24.5 ± 0.1	21.1	20.9		
	β -CH	10. \pm 1	24.9 ± 0.1	22.3	22.2		
	all	14.2 ± 0.6^{e}					

 $^a\Delta G_{353}^{\dagger}(\text{exp})$ are the experimental values, and $\Delta G_{298}^{\dagger}(\text{DFT/gas phase})$ and $\Delta G_{298}^{\dagger}(\text{DFT/TFE})$ are calculated by DFT for the gas phase and TFE solutions, respectively. b Calculated using initial reaction rates at <10% substrate conversion. c Weighted average for o- and p-CH bonds, $k_{c,o-p}$. d Not determined due to the difficulty of locating t S_{Ar-X} in TFE. c Weighted-average value for all t C(sp²)-H bonds, t C-all.

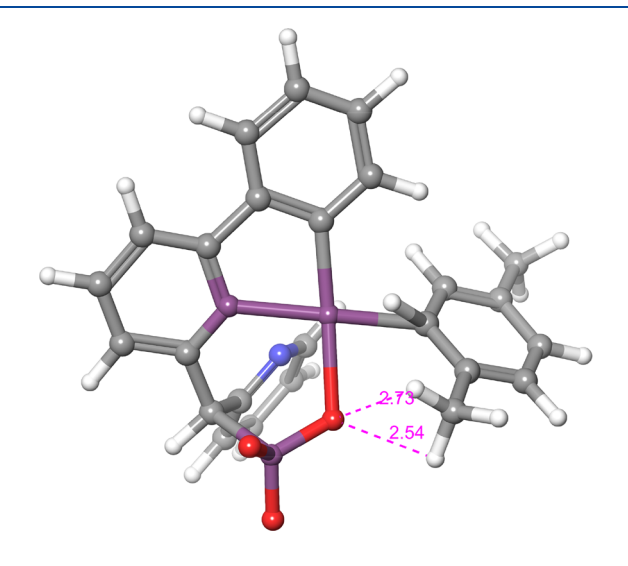


Figure 2. DFT-optimized structure of the transition state TS_{Ar-X} for the oxidative addition of a *p*-xylene $C(sp^2)$ -H bond. The distances (Å) between the pincer ligand oxygen atom and two hydrogen atoms of one of the substrate's methyl groups are shown.

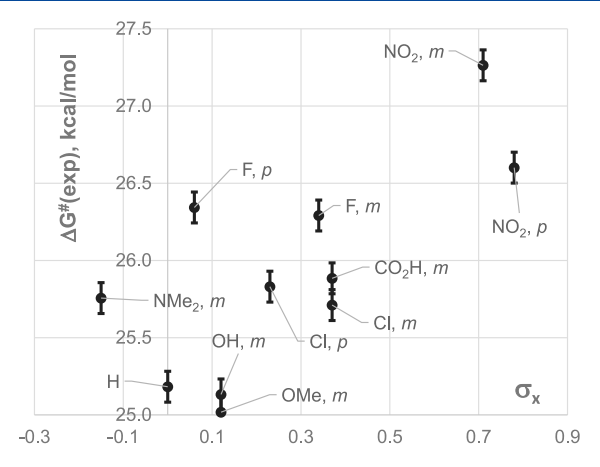


Figure 3. Plot of Gibbs energies of activation of reaction 1 involving m- and p-CH bonds of monosubstituted benzene derivatives 7, 9–12, 14, and 15 and the substituents' Hammett $\sigma_{\rm X}$ constants.

Similarly to phenol and anisole, benzodioxole (8) (Table 1), containing a methylenedioxo fragment, is more reactive than

benzene. These observations suggest that the catalyst 1 may be weakly electrophilic overall.

The lack of a good correlation in Figure 3 may not be surprising. The regular $\sigma_{\rm X}$ constants are determined from proton transfer equilibria (p K_2 values) of the corresponding Xsubstituted benzoic acids, where the electron density change on the carboxylic group bearing arene carbon atom is responsible for the reactivity change ("charge control"). ¹⁴ In turn, on the basis of the classic mechanistic consideration of concerted CH oxidative addition to a transition-metal center such as one involving TS_{Ar-X} (Figure 2), such reactions are orbital-controlled and, ideally, involve a concerted transfer of two electrons from the metal d subshell to the σ^* orbital of the substrate C-H bond and a two-electron transfer of the substrate C-H σ -bond electrons onto a suitable empty metal orbital. 15 Hence, the CH bond oxidative addition to a metal center represents a substantially different reaction type that may require the use of a different type of substituent $\sigma_{\rm X}$ constants (vide infra). The involvement of two oppositely directed electron flows in C(sp²)-H bond oxidative addition reactions may result in the absence of a strong dependence between the reactivity of X-substituted substrates and $\sigma_{\rm X}$ constants, as observed in Figure 3. Still, in some situations, the reaction activation energy may be more sensitive to either "electrophilicity" or "nucleophilicity" of the engaging CH bond, depending on the nature and the orbital parameters of the reacting species.

In this situation, we turned to DFT modeling of the reaction rate-limiting step and calculations of the Gibbs energy of the corresponding transition states TS_{Ar-X} to help account for the available experimental observations.

2.5. DFT Modeling of the Effect of Substituents on the Kinetics of H/D Exchange Catalyzed by Complex 1. The Gibbs energies of the formation of the respective transition states TS_{Ar-X} from 1 and the corresponding substrates (eq 5) were calculated in this work using the DFT method employing a PBE¹⁶ functional and a relativistic LACVP** basis set, as implemented in the Jaguar program package,¹⁷ as was done in our previous DFT analysis of reaction 1 with benzene as a substrate:⁴

$$1 + Ar - X \rightarrow \{TS_{Ar-X}\}^{\ddagger} + H_2O \quad \Delta G_{298}^{\ddagger}$$
 (5)

In addition to the gas phase geometry optimization at the PBE/LACVP** level of theory with a full frequency analysis resulting in the corresponding gas phase values $\Delta G_{298}^{\dagger}(\mathrm{DFT}/$ gas phase), geometry optimizations were also done for TFE solutions utilizing Poisson-Boltzmann continuum solvation model (PBF), resulting in the corresponding solution phase values, ΔG_{298}^{\dagger} (DFT/TFE). Due to some difficulties at geometry optimization of the transition states in TFE, some conformationally more flexible substrates were not characterized in the liquid phase. The so-produced DFT-calculated Gibbs energies of activation, $\Delta G_{298}^{\ddagger}(\mathrm{DFT/gas}\ \mathrm{phase})$ and ΔG_{298}^{\dagger} (DFT/TFE), are given in Table 1 for m-CH and p-CH bonds of monosubstituted benzene derivatives 7, 9-12, 14, and 15, α - and β -CH bonds of thiophene (16), and σ -CH bonds of fluorobenzene (11), chlorobenzene (12), and pxylene (5).

From the calculated gas-phase values, $\Delta G_{298}^{\dagger}(\mathrm{DFT/gas})$ phase), and the corresponding calculated TFE solution values, $\Delta G_{298}^{\dagger}(\mathrm{DFT/TFE})$, given in the last two columns in Table 1, one can note that in most cases they differ only by 0.1–0.4 kcal/mol. Hence, the calculated solvation effects in reaction 5

are small. The corresponding higher-temperature values, $\Delta G_{353}^{\dagger}(\mathrm{DFT/gas}\ \mathrm{phase})$ and $\Delta G_{353}^{\dagger}(\mathrm{DFT/TFE})$, have also been found in our calculations (Tables S1 and S2). These values follow the same trend (Figure S19), in comparison to $\Delta G_{298}^{\dagger}(\mathrm{DFT/gas}\ \mathrm{phase})$ and $\Delta G_{298}^{\dagger}(\mathrm{DFT/TFE})$ values discussed next.

On the basis of the results of our previous work, our DFT calculations of reaction 5 with complex 1 as a reference compound underestimate the experimental values of the reaction Gibbs energy of activation by $\sim 2-3$ kcal/mol. This discrepancy is related to the fact that in neat TFE solutions complex 1 produces an unknown/not isolable adduct with the solvent in a slightly exergonic reaction.⁴ Hence, for more accurate results, not complex 1 but its TFE adduct should be viewed as a reference state. This consideration suggests that the same small correction parameter needs to be added to each of the DFT-calculated Gibbs energies of activation, $\Delta G_{298}^{\ddagger}(\mathrm{DFT/gas}\ \mathrm{phase})$ or $\Delta G_{298}^{\ddagger}(\mathrm{DFT/TFE})$, when they are compared with the experimental values $\Delta G_{353}^{\ddagger}(\mathrm{exp})$. With this idea in mind, a good match of the Gibbs energies of activation calculated for the gas-phase reactions, ΔG_{298}^{\dagger} (DFT/ gas phase), and the experimental values, $\Delta G_{353}^{\dagger}(\exp)$, can be obtained when the former values are corrected (increased) by 2.3 kcal/mol (Figure 4a; the solid line with slope 1). Two types of CH bonds, p-xylene C(sp2)-H bonds and

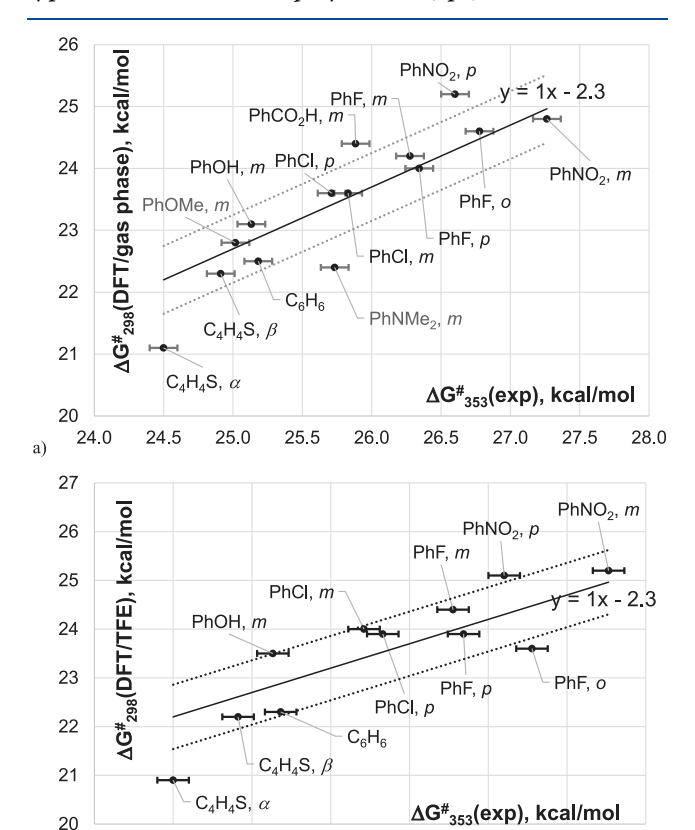


Figure 4. Plot of the DFT-calculated Gibbs energies of activation of reaction 5 vs the experimental values $\Delta G_{353}^{\ \pm}(\exp)$: (a) the gas-phase calculated $\Delta G_{298}^{\ \pm}(\mathrm{DFT/gas})$ phase); (b) the TFE calculated $\Delta G_{298}^{\ \pm}(\mathrm{DFT/TFE})$. Solid lines are shown for minimal root-mean-square deviations of the "corrected" DFT-calculated data from the experimental data with the slope set to 1. Dashed lines are spaced at the RMS value from the solid lines. Strongly deviating data points for p-xylene and chlorobenzene o-CH bonds are not shown.

25.5

26.0

24.0

24.5

25.0

26.5

27.0

27.5

chlorobenzene o-CH bonds, are not included in this correlation, as the steric effects of the substituents in these substrates, Me and Cl, appear to be overestimated in our DFT calculations of the reaction 5 Gibbs energy of activation (vide infra). The 2.3 kcal/mol correction allows us to attain the rootmean-square deviation (RMS) of the DFT-calculated corrected values from the experimental values of 0.5 kcal/mol, which is small, in comparison to some typical accuracies attainable currently in DFT calculations of organometallic reactions. 18 In turn, the data points for p-xylene and chlorobenzene o-CH bonds deviate from the solid line on the plot in Figure 4a by 4.2 and 5.7 kcal/mol, respectively, both being greater than three RMS values. Interestingly, a more "compact" fluorine substituent does not exhibit such issues. The use of a dispersion-corrected DFT functional PBE-D3¹⁹ for singlepoint calculations corresponding to the level of theory PBE-D3/LACVP**//PBE/LACVP** results only in a minor improvement in this respect (see Tables S3-S6 and Figures S20 and S21).

With the exception of thiophene α -CH bonds and N,N-dimethylaniline m-CH bonds, the remaining data in Figure 4a fall into a relatively narrow range $\Delta G_{353}^{\ddagger}(\exp) - 2.3 \pm \text{RMS}$ (RMS = 0.5 kcal/mol); this range is shown in Figure 4a with two dashed lines with slope 1 each. The point corresponding to N,N-dimethylaniline may be slightly off of the trend as a consequence of the ability of this compound to become involved in an acid—base equilibrium with TFE, so that a sizable part of N,N-dimethylaniline is converted to the corresponding cation, which has a different reactivity that is not accounted for in our DFT modeling. Qualitatively, the cation derived from N,N-dimethylaniline should be more electron poor than the aniline itself and, on the basis of the overall reactivity trend mentioned earlier, be less reactive.

Turning now to the DFT-calculated Gibbs energies of activation of reaction 5 in TFE solutions, ΔG_{298}^{\dagger} (DFT/TFE), and holding in mind small solvation effects calculated for reaction 5, as noted earlier, we can obtain an expected good match of the calculated values and the experimental values, ΔG_{353}^{\dagger} (exp), when the former values are corrected (increased) by 2.3 kcal/mol (Figure 4b; the solid line with slope 1). The root-mean-square deviation of the DFT-calculated corrected values from the experimental values is 0.7 kcal/mol (Figure 4b). Once again, a significant deviation from the solid line in Figure 4b of the calculated values $\Delta G_{298}^{\dagger}(DFT/TFE)$ for pxylene and chlorobenzene o-CH bonds, by 4.7 and 5.1 kcal/ mol, respectively, may suggest that the DFT model used here overestimates the steric effects of the Me and Cl fragment in these substrates in our calculations of the Gibbs energy of activation of reaction 5.

2.6. Novel Hammett Constants σ_X^M for Metal-Assisted C–H Bond Activation Reactions. The inability to describe substituent effects in the organometallic reaction (5) using Hammett σ_X constants and the somewhat limited accuracy of modern DFT calculations, as demonstrated in Figure 4 and shown by other researchers, ¹⁸ prompted us to introduce a new empirical set of Hammett constants, σ_X^M , for metal-assisted CH bond activation reactions. Such constants may be useful in analyzing the reactivity of various metal complexes and substrates in CH activation reactions. Our σ_X^M constants are defined by eq 6. Since reaction 5 is decelerated by electron-withdrawing groups, for the sake of consistency of the sign of σ_X^M values and the sign of classical σ_X values for the same

substituent X, the negative sign is used in front of the logarithmic function:

$$\sigma_{\mathbf{X}}^{\mathbf{M}} = -\log(k_{c}(\mathbf{X})/k_{c}(\mathbf{H})) \tag{6}$$

The corresponding σ_X^M values are given in Table 2. Except NMe₂ group, the series of σ_X^M constants in Table 2 is

Table 2. Hammett-Type $\sigma_{\rm X}^{\ \ M}$ Constants for Metal-Assisted C–H Bond Activation Reactions Based on Rate Constant $k_{\rm c}$ Data from Table 1

	substituent X								
	OMe	ОН	Н	Cl	CO ₂ H	F	NO ₂		
$\sigma_{\rm X}^{\ \ m M}$, meta	-0.10	-0.03	0	0.33	0.43	0.68	1.29		
$\sigma_{\!\scriptscriptstyle m X}^{ m M}$, para			0	0.40		0.72	0.88		

qualitatively similar to that of σ_X values. An unexpectedly large positive value was calculated for the NMe₂ group, 0.34 (not shown in Table 2), which may be related to the group's partial protonation in TFE solutions, and therefore, this value is not recommended for general use.

2.7. Regioselectivity of H/D Exchange (Reaction 1). Notably, the initial regioselectivity of the H/D exchange observed in reaction 1 typically is low, as follows from an inspection of the rate constants $k_{\rm c}$ given in Table 1. For example, for chlorobenzene the $k_{\rm c,o}$ (ortho-CH bonds), $k_{\rm c,m}$ (meta-CH bonds), and $k_{\rm c,p}$ (para-CH bonds) values fall in a narrow range of 2.2–3.2 M⁻¹ h⁻¹. For fluorobenzene the reaction rate constant for o-CH bonds, $k_{\rm c,o}=0.7$ M⁻¹ h⁻¹, is only 2 times lower than the value for its m-CH bonds, $k_{\rm c,m}=1.3$ M⁻¹ h⁻¹, or p-CH bonds, $k_{\rm c,p}=1.43$ M⁻¹ h⁻¹, which, in turn, are very similar.

There are a few notable exceptions from this "low selectivity" picture. In particular, nitrobenzene o-CH bonds are virtually unreactive under our reaction conditions, presumably due to both the electronic and steric effects of this group, whereas the p-CH bonds, $k_{\rm c,p} = 0.9~{\rm M}^{-1}~{\rm h}^{-1}$, are somewhat more reactive than the meta-CH bonds, $k_{\rm c,m} = 0.35~{\rm M}^{-1}~{\rm h}^{-1}$.

Two other substrates demonstrating notable positional selectivity in their CH bond deuteration (1) are N,N-dimethylaniline and indole. The relatively low reactivity of m-CH bonds of N,N-dimethylaniline makes it possible to carry out a selective deuteration of the CH bonds in the ortho and para positions of this substrate after 27 h of the reaction (Figure 5). An exclusive deuteration of the indole β -CH bonds with a virtually statistical 88% degree of deuterium incorporation was observed in our experiments for indole (17) after 45 min of reaction.

To illustrate qualitatively some possible reasons behind the observed (often low) regioselectivity of complex 1 in the H/D exchange reaction (1) that would be consistent with the proposed reaction mechanism (Scheme 2), we considered the following two cases, one involving deuteration of α - vs β -CH bonds of thiophene (TP) and another involving deuteration of the m- vs p-CH bonds of nitrobenzene (NB). Experimentally, the deuteration of thiophene α -CH bonds and the deuteration of nitrobenzene p-CH bonds is slightly selective (Table 1 and Chart 2). For thiophene the difference in the reactivity of α - and β -CH bonds is reproduced qualitatively in our DFT calculations of the Gibbs energy of activation of reaction 5; for nitrobenzene the DFT predicts virtually no difference (Table 1 and Figure 4).

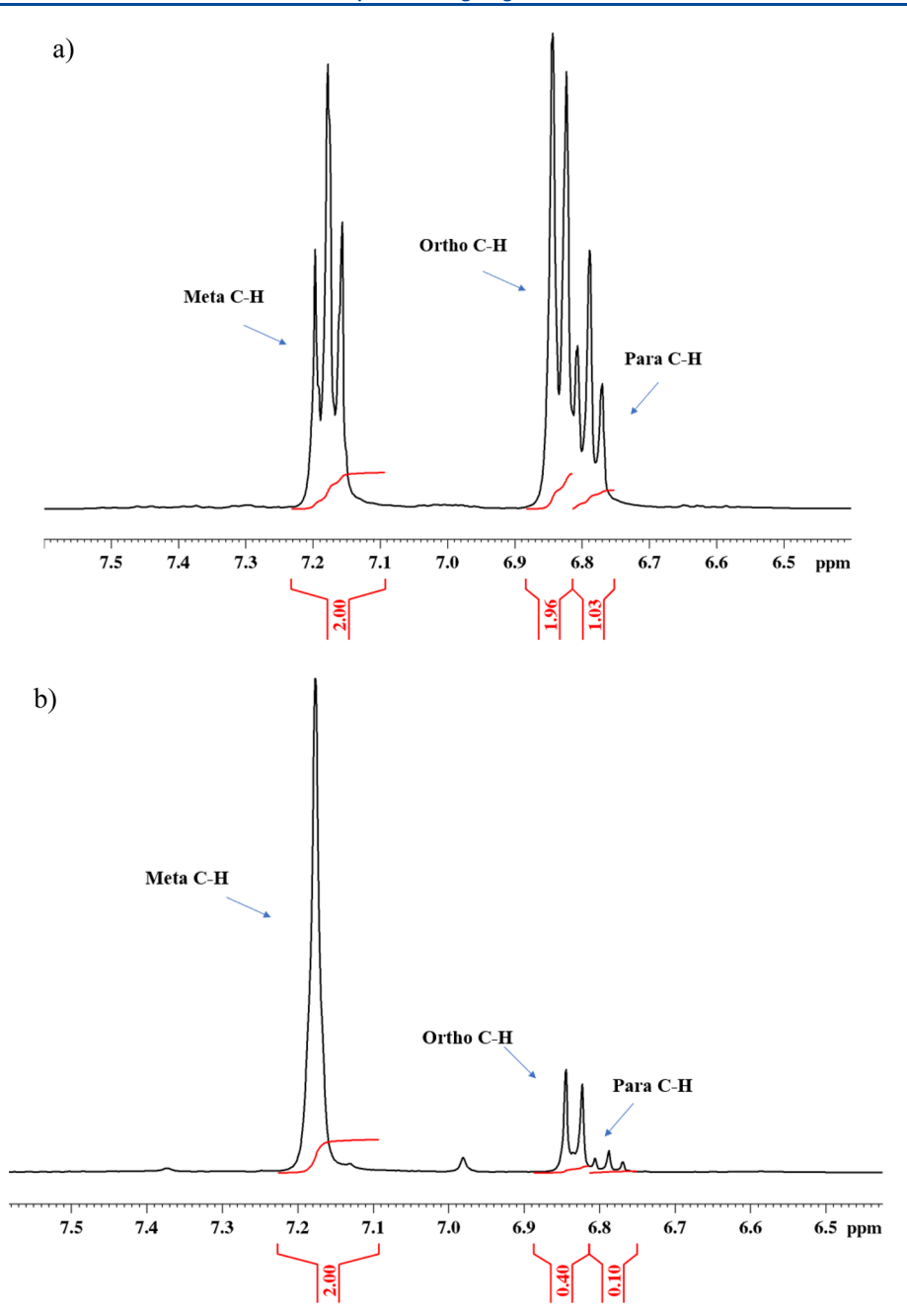


Figure 5. 1 H NMR spectra (aromatic region) demonstrating the selectivity of the H/D exchange between N,N-dimethylaniline and wet TFE- d_1 catalyzed by complex 1 at 80 $^{\circ}$ C: (a) before reaction; (b) after 27 h.

To that end, we considered a perturbation molecular orbital theory approach²⁰ where the two fragments LPt and the corresponding CH bond of thiophene or nitrobenzene are, formally, engaged in the interaction in the corresponding transition states TS_{Ar-X}. First, we consider the difference in the charges on the atoms of competing CH bonds involved in the reaction. The DFT-calculated natural charge on the Pt atom in the LPt fragment is positive, 0.69. Hence, a larger negative charge on the carbon atom of a reacting CH bond would lead to a stronger interaction of LPt and the CH bond, a greater stabilization of the corresponding TS_{Ar-X}, a lower activation energy, and a higher selectivity with respect to that type of CH bond. In turn, in the absence of a significant difference in the charge on the carbon atoms of the competing CH bonds, we focus on the covalent component of such an interaction. A

stronger interaction of the frontier molecular orbitals (FMOs) of these fragments, which is proportional to the square of the FMO resonance integral and inversely proportional to their energy difference,²⁰ would favor a lower activation barrier.

Considering the natural charges on the carbon atoms of the thiophene α -CH bond, -0.47, and β -CH bond, -0.30 (the natural charges on the hydrogen atoms are virtually identical, +0.26), we can expect a somewhat selective activation of the substrate's α -CH bonds. In turn, on qualitative comparison of the two FMO diagrams in Figure 6, one involving thiophene's α -CH bonds (Figure 6a) and one involving thiophene's β -CH bonds (Figure 6b), no dramatic difference is expected in terms of the energy of interactions of the FMOs of the engaged fragments in these two cases. On the one hand, $\Delta E_{2,a}$ (Figure 6a) corresponding to the reaction involving the thiophene α -

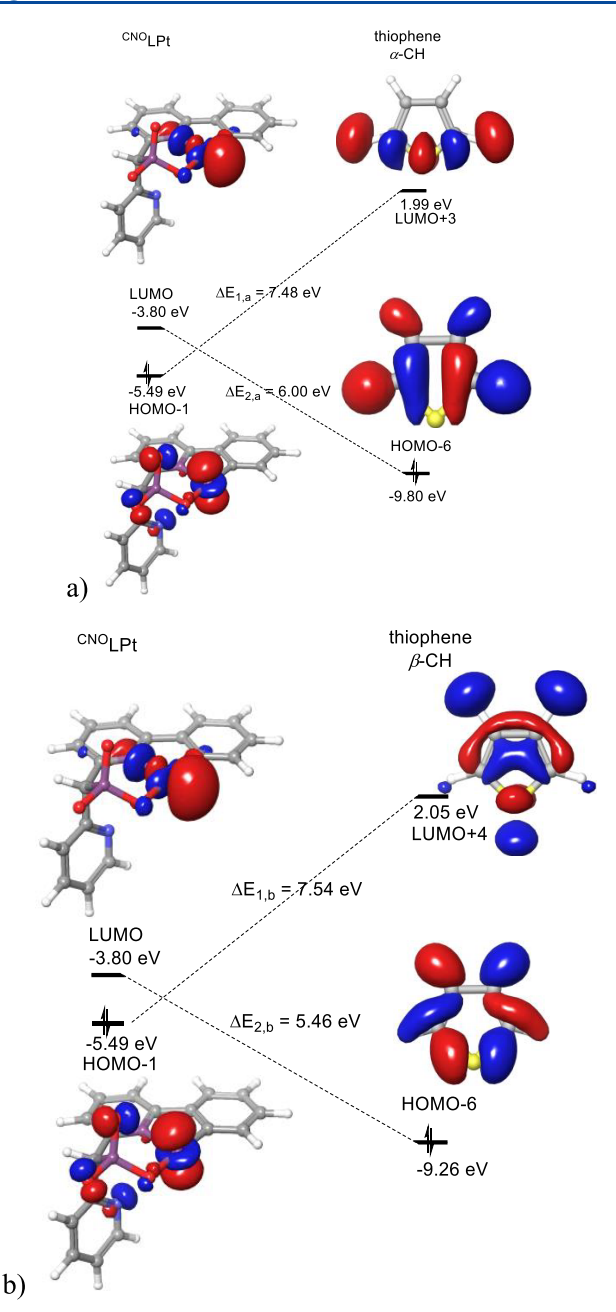


Figure 6. Qualitative frontier molecular orbital diagrams illustrating FMO interactions between frontier orbitals of the LPt fragment and the corresponding C–H bonds of thiophene: (a) α -CH bonds of thiophene; (b) β -CH bonds of thiophene.

CH bond is slightly greater than $\Delta E_{2,b}$ (Figure 6b) corresponding to the reaction of the thiophene β -CH bond. On the other hand, the α -CH HOMO is more localized between the bonded α -C and H atoms, thus favoring a slightly stronger interaction of the α -CH HOMO with the LUMO of the LPt fragment. Therefore, we can speculate that the latter orbital interactions may favor a lower energy of activation and a faster α -CH bond cleavage, thus reinforcing the effect of the Coulombic interactions. Overall, this qualitative perturbation molecular orbital theory analysis predicts a faster cleavage of the thiophene's α -CH bonds, as observed, with $k_{c,\alpha}=18~{\rm M}^{-1}~{\rm h}^{-1}$ and $k_{c,\beta}=10~{\rm M}^{-1}~{\rm h}^{-1}$ (Table 1). Also, the above discussion of the importance of the Coulombic interactions between the

LPt and CH bond fragments in this reaction points to a somewhat electrophilic character of complex 1.

Considering now the m- and p-CH bonds of free nitrobenzene, we find virtually identical natural charges on the H atoms,+0.26, and very similar natural charges on the m- and p-C atoms, -0.24 and -0.22, respectively. Hence, we can expect that the Coulombic interactions of the fragments do not affect the reaction 1 selectivity involving this substrate. In turn, on qualitative comparison of two FMO diagrams in Figure 7,

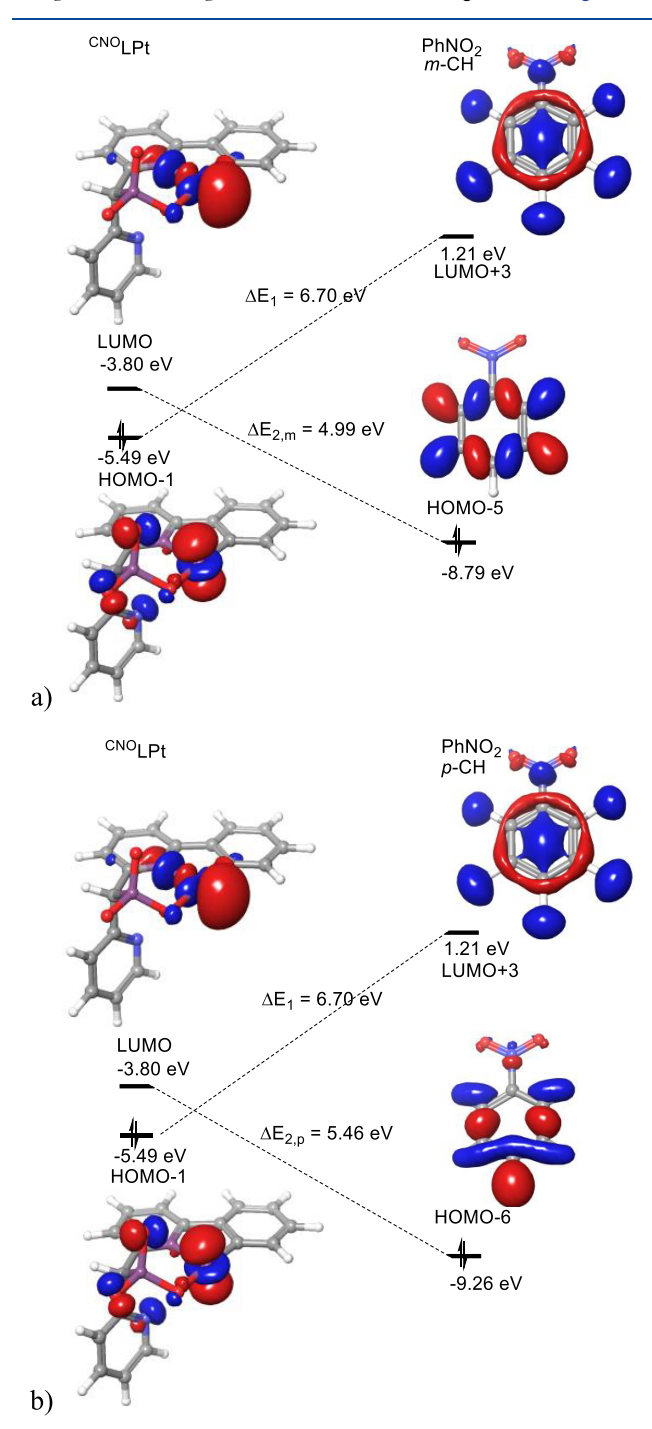


Figure 7. Qualitative frontier molecular orbital diagrams illustrating FMO interactions between frontier orbitals of the LPt fragment and the corresponding C-H bonds of nitrobenzene: (a) m-CH bonds of nitrobenzene; (b) p-CH bonds of nitrobenzene.

one involving nitrobenzene's m-CH bonds (Figure 7a) and one involving nitrobenzene's p-CH bonds (Figure 7b), two hypotheses can be made. First, in both cases the LPt_{IJIMO}- NB_{HOMO} gap, ΔE_2 , is smaller than the $LPt_{HOMO} - NB_{LUMO}$ gap, ΔE_1 , thus suggesting that the first interaction may be more important and the LPt fragment is somewhat electrophilic in its behavior even with respect to electron-poor nitrobenzene. Second, the HOMO-LUMO energy gap $\Delta E_{2,p}$ (Figure 7b) corresponding to the reaction involving the nitrobenzene p-CH bond is slightly greater than $\Delta E_{2,m}$ (Figure 7a) corresponding to the cleavage of the nitrobenzene m-CH bond. At the same time, the p-CH HOMO is more localized between the bonded p-C and -H atoms, allowing for a better orbital overlap of the p-CH HOMO with the LPt LUMO. Hence, we speculate that the latter factor is more important. Therefore, this qualitative perturbation molecular orbital theory analysis suggests an "orbital-controlled" slight kinetic preference of the p-CH bond cleavage, as observed experimentally: $k_{c,p} = 0.9 \text{ M}^{-1} \text{ h}^{-1} \text{ vs } k_{c,m} = 0.35 \text{ M}^{-1} \text{ h}^{-1}$.

Overall, depending on the type of a CH bond donor and the nature of a metal fragment engaged in a reaction, one needs to consider the contributions to the reaction activation energy of the Coulombic interactions of the fragments (ultimately, a "charge controlled" reactivity) and/or their FMO interactions (ultimately, "orbital-controlled" reactivity). Driven by this conclusion, we found that, similar to the case for thiophene, in reaction 1 involving indole the observed exclusive selectivity with respect to the substrate's β -CH vs α -CH bonds is likely a consequence of the enhanced Coulombic interactions of the LPt and β -CH bond fragments ("charge control"): the natural charge on the indole β -C atom is -0.32, in comparison to -0.06 on its α -C atom, and the natural charges on the respective hydrogen atoms are almost identical, 0.26 and 0.24.

The results of our analysis of the reaction 1 selectivity involving complex 1 would be interesting to compare with those of other transition-metal-based systems. Although it may be valuable for some practical applications,³ in general, the kinetic selectivity of H/D exchange in substituted benzenes has not been systematically analyzed in previous works. In turn, the practically important extent and selectivity of deuteration of aromatic substrates at the late stage of the reaction have been reported for some catalytic systems^{7,9} and can be compared with our results included in Chart 2.

In one of the recent works, the anionic rhodium(III) complex Na[(bpzmc)RhCl₃] (36; Chart 5) in combination

Chart 5. Rh(III) Complex 36 Used in Combination with 3 Equiv of AgOTf for Catalytic H/D Exchange between Substituted Benzene Substrates and CF₃CO₂D at 100 °C⁹

with 3 equiv of AgOTf was used as a catalyst in H/D exchange between a number of aromatic substrates and CF₃CO₂D at 100 °C. The CH activation in this system was proposed to operate by a concerted metalation—deprotonation mechanism, which

is distinct from CH bond oxidative addition to a Pt(II) center in this work.

A qualitative comparison of the extent of deuteration x in Chart 2 with that for identical substrates after 24 h of reaction reported in ref 9 shows some similarities and some differences. For example, for one of the more reactive substrates, anisole (7), after 28 h of reaction the catalyst 1 allows for a lower extent of o-CH deuteration (31%), in comparison to 36/AgOTf (77%), whereas the extent of deuteration of m- and p-CH bonds is about the same, 53–62% in the presence of complex 1/TFE- d_1 and 64% (on average) in the 36/AgOTf/CF₃CO₂D system.

For another reactive substrate, phenol (9), after 24 h of reaction both systems show almost identical performance and the lack of selectivity with respect to phenol's *o-, m-,* or *p-*CH bonds: 67% deuteration for *o-*CH and 69% deuteration, on average, for *m-* and *p-*CH bonds for complex 1/TFE-*d*₁ system vs 55% (*o-*CH) and 62% (*m-* and *p-*CH bond average) for the complex 35/AgOTf/CF₃CO₂D system.

Notably, the reactivity of N_iN -dimethylaniline (10,)is higher when the less acidic system $1/\text{TFE-}d_1$ is employed, in comparison to the $35/\text{AgOTf/CF}_3\text{CO}_2\text{D}$ system. In particular, after 25 h of reaction with $1/\text{TFE-}d_1$ the extent of deuteration of the substrate's m-CH bonds is 14%; it is 75% for o-CH bonds and 77% for p-CH bonds, which corresponds to 51%, on average, for all of the substrate $C(\text{sp}^2)$ —H bonds. In turn, a 25% average extent of deuteration was achieved with $35/\text{AgOTf/CF}_3\text{CO}_2\text{D}$. It appears that the protonation of the basic dimethylamino fragment of 10 transforms it into an electron-withdrawing ammonium group, thus causing the reaction to slow.

Interestingly, a higher extent of deuteration by the complex $1/\mathrm{TFE}$ - d_1 system, in comparison to $35/\mathrm{AgOTf/CF_3CO_2D}$, was observed after similar reaction times for electron-poor chlorobenzene. The average degree of deuteration for all arene $\mathrm{C}(\mathrm{sp^2})\mathrm{-H}$ bonds is 39% in the first system and 2.6% in the second system.

2.8. Ibuprofen and Naproxen Substrates. Driven by curiosity as to whether our 1/TFE- d_1 system can be used for deuteration of some pharmaceutical compounds containing $C(sp^2)$ -H bonds, we tested two over the counter medications, ibuprofen (33) and naproxen (34) (Chart 4). Due to their low solubility in TFE, a 1/1 (v/v) mixture of wet TFE- d_1 and CDCl₃ was used instead. The resulting homogeneous solutions containing catalyst 1 were subjected to the reaction at 80 °C. Similar to the reaction involving benzoic acid, a fine yellow precipitate was observed in ibuprofen-containing solutions already after 3 h. At this time the reaction was stopped to reveal a negligible (<2%) deuterium incorporation. The probable reasons behind this low reactivity are the rapid catalyst deactivation and some steric interference between the catalyst and the substituents present in this substrate which are in a position ortho to the available $C(sp^2)$ -H bonds. In the case of naproxen the catalyst deactivation was also observed but only after 20 h and the reaction resulted in an average 9% deuterium incorporation per $C(sp^2)$ -H bond with a low overall selectivity with respect to six distinct types of CH bonds (Chart 4). This result shows some promise of a future possible application of the $1/\text{TFE-}d_1$ system for deuteration of some pharmaceutical compounds containing aromatic CH bonds.

CONCLUSION

As a result of this work, a wide range of arene substrates were tested in catalytic H/D exchange with TFE-d₁ solvent catalyzed by the Pt(II) pincer complex 1 (Charts 2-4). (Het)arene substrates and their derivatives with relatively weekly coordinating functional groups can be efficiently deuterated (Chart 2), whereas substrates that are either not chemically robust in the presence of 1, or strongly coordinate 1, or too electron poor cannot be deuterated (Chart 3). By monitoring the initial stage of the H/D exchange, we were able to measure the corresponding initial reaction rates and, often, characterize the reaction kinetics selectively for different types of C(sp²)-H bonds involved (Table 1). A moderate to very high positional kinetic selectivity was observed for a few substrates, N,N-dimethylaniline, nitrobenzene, and indole, whereas for the rest of the substrates the selectivity is low. An almost "statistical" deuterium distribution between the substrate reactive $C(sp^2)$ -H bonds and TFE- d_1 solvent that corresponds to 67-88% deuterium incorporation could be achieved for the most active compounds, phenol, indole, and N,N-dimethylaniline, after 45 min (indole) to 24 h. An attempt to use the 1/TFE-d₁/CDCl₃ system for deuteration of the pharmaceutical compounds ibuprofen and naproxen (Chart 4) was only successful for the latter, which has relatively unencumbered C(sp²)-H bonds, albeit with a low 9% average deuterium incorporation after 20 h, which still may be an acceptable level in some labeling experiments.³ Notably, our attempts to correlate the Gibbs energies of activation of the H/ D exchange involving X-monosubstituted benzene derivatives with the corresponding Hammett meta and para σ_X constants resulted in a lack of good correlation and prompted us to introduce a new set of empirical Hammett constants, $\sigma_{\rm X}^{\rm M}$, which may be useful in the future research of metal-assisted C-H bond activation reactions. Finally, a DFT modeling of the H/D exchange reaction demonstrates a satisfactory match of the experimentally found and calculated Gibbs energies of activation for the reactions involving m- and p-CH bonds of substituted benzenes, as well as the CH bonds of thiophene.

ASSOCIATED CONTENT

Supporting Information

The Supporting Information is available free of charge on the ACS Publications Web site at DOI: (PDF and XYZ). The Supporting Information is available free of charge at https://pubs.acs.org/doi/10.1021/acs.organomet.0c00652.

NMR spectra and computational details (PDF)
Cartesian coordinates of the calculated structures (XYZ)

AUTHOR INFORMATION

Corresponding Author

Andrei N. Vedernikov – Department of Chemistry and Biochemistry, University of Maryland, College Park, Maryland 20742, United States; ocid.org/0000-0002-7371-793X; Email: avederni@umd.edu

Authors

Morgan Kramer – Department of Chemistry and Biochemistry, University of Maryland, College Park, Maryland 20742, United States

David Watts – Department of Chemistry and Biochemistry, University of Maryland, College Park, Maryland 20742, United States Complete contact information is available at: https://pubs.acs.org/10.1021/acs.organomet.0c00652

Notes

The authors declare no competing financial interest.

ACKNOWLEDGMENTS

This work was supported by the National Science Foundation (CHE-1800089). The authors thank Dr. Phil DeShong for the idea of possible applications of complex 1 for the catalytic deuteration of pharmaceuticals.

REFERENCES

- (1) Garnett, J. L.; Hodges, R. J. Homogeneous Metal-Catalyzed Exchange of Aromatic Compounds. A New General Isotopic Hydrogen Labeling Procedure. *J. Am. Chem. Soc.* **1967**, *89*, 4546–4547.
- (2) (a) Shilov, A. E.; Shulpin, G. B. Activation and Catalytic Reactions of Saturated Hydrocarbons in the Presence of Metal Complexes; Kluwer: Boston, 2000. (b) Labinger, J. A.; Bercaw, J. E. Mechanistic Studies of the Shilov System: a Retrospective. J. Organomet. Chem. 2015, 793, 47–53.
- (3) Atzrodt, J.; Derdau, V.; Kerr, W. J.; Reid, M. C-H Functionalisation for Hydrogen Isotope Exchange. *Angew. Chem., Int. Ed.* **2018**, *57*, 3022–3047.
- (4) Watts, D.; Wang, D.; Adelberg, M.; Zavalij, P. Y.; Vedernikov, A. N. C-H and O_2 Activation at a Pt(II) Center Enabled by a Novel Sulfonated CNN Pincer Ligand. Organometallics 2017, 36, 207–219.
- (5) Watts, D.; Wang, D.; Zavalij, P. Y.; Vedernikov, A. N. Novel Sulfonated CNN Pincer Ligands for Facile C-H Activation at a Pt(II) Center. *Isr. J. Chem.* **2017**, *57*, 1010–1022.
- (6) (a) Ziatdinov, V. R.; Oxgaard, J.; Mironov, O. A.; Young, K. J. H.; Goddard, W. A.; Periana, R. A. Carboxylic Solvents and O-Donor Ligand Effects on CH Activation by Pt(II). *J. Am. Chem. Soc.* 2006, 128, 7404–7405. (b) Young, K. J. H.; Meier, S. K.; Gonzales, J. M.; Oxgaard, J.; Goddard, W. A.; Periana, R. A. Heterolytic CH Activation with a Cyclometalated Platinum(II) 6-Phenyl-4,4'-di-tert-butyl-2,2-Bipyridine Complex. *Organometallics* 2006, 25, 4734–4737. (c) Hickman, A. J.; Villalobos, J. M.; Sanford, M. S. Quantitative Assay for the Direct Comparison of Platinum Catalysts in Benzene H/D Exchange. *Organometallics* 2009, 28, 5316–5322. (d) Hickman, A. J.; Cismesia, M. A.; Sanford, M. S. Structure Activity Relationship Study of Diimine Pt^{II} Catalysts for H/D Exchange. *Organometallics* 2012, 31, 1761–1766.
- (7) Emmert, M. H.; Gary, J. B.; Villalobos, J. M.; Sanford, M. S. Platinum and Palladium Complexes Containing Cationic Ligands as Catalysts for Arene H/D Exchange and Oxidation. *Angew. Chem., Int. Ed.* **2010**, *49*, 5884–5886.
- (8) Watts, D.; Zavalij, P. Y.; Vedernikov, A. N. Consecutive C-H and O₂ Activation at a Pt(II) Center to Produce Pt(IV) Aryls. *Organometallics* **2018**, *37*, 4177–4180.
- (9) Rhinehart, J. L.; Manbeck, K. A.; Buzak, S. K.; Lippa, G. M.; Brennessel, W. W.; Goldberg, K. I.; Jones, W. D. Catalytic Arene H/D Exchange with Novel Rhodium and Iridium Complexes. *Organometallics* **2012**, *31*, 1943–1952.
- (10) (a) Jones, W. D. Alkane Activation Processes by Cyclopentadienyl Complexes of Rhodium, Iridium, and Related Species. In *Activation and Functionalization of Alkanes*; Hill, C., Ed.; Wiley: New York, 1989; pp 111–149. (b) Jiao, Y.; Morris, J.; Brennessel, W. W.; Jones, W. D. Kinetic and Thermodynamic Selectivity of Intermolecular C-H Activation at [Tp'Rh(PMe₃)]. How Does the Ancillary Ligand Affect the Metal-Carbon Bond Strength? *J. Am. Chem. Soc.* **2013**, 135, 16198–16212.
- (11) Eisenstein, O.; Milani, J.; Perutz, R. N. Selectivity of C-H Activation and Competition between C-H and C-F Bond Activation at Fluorocarbons. *Chem. Rev.* **2017**, *117*, 8710–8753.
- (12) (a) Ma, S.; Villa, G.; Thuy-Boun, P. S.; Homs, A.; Yu, J.-Q. Palladium-catalyzed ortho-selective C-H deuteration of arenes:

evidence for superior reactivity of weakly coordinated palladacycles. *Angew. Chem., Int. Ed.* **2014**, *53*, 734–737. (b) Bag, S.; Petzold, M.; Sur, A.; Bhowmick, S.; Werz, D. B.; Maiti, D. Palladium-Catalyzed Selective *meta*-C-H Deuteration of Arenes: Reaction Design and Applications. *Chem. - Eur. J.* **2019**, *25*, 9433–9437. (c) Janni, M.; Peruncheralathan, S. Catalytic selective deuteration of halo(hetero) arenes. *Org. Biomol. Chem.* **2016**, *14*, 3091–3097.

- (13) Anslyn, E. V.; Dougherty, D. A. Modern physical organic chemistry; University Science Books: Sausalito, CA, 2006; p 609.
- (14) Huang, Y.; Liu, L.; Liu, W.; Liu, S.; Liu, S. Modeling Molecular Acidity with Electronic Properties and Hammett Constants for Substituted Benzoic Acids. *J. Phys. Chem. A* **2011**, *115*, 14697–14707.
- (15) Hartwig, J. F. The Organotransition Metal Chemistry: From Bonding to Catalysis; University Science Books: Sausalito, CA, 2010.
- (16) Perdew, J. P.; Burke, K.; Ernzerhof, M. Generalized gradient approximation made simple. *Phys. Rev. Lett.* **1996**, *77*, 3865–3868.
- (17) Jaguar, ver. 8.4; Schrödinger, LLC: New York, NY, 2014.
- (18) Hopmann, K. H. How Accurate is DFT for Iridium-Mediated Chemistry? *Organometallics* **2016**, *35*, 3795–3807.
- (19) Grimme, S.; Antony, J.; Ehrlich, S.; Krieg, H. A consistent and accurate *ab initio* parametrization of density functional dispersion correction (DFT-D) for the 94 elements H-Pu. *J. Chem. Phys.* **2010**, 132, 154104.
- (20) (a) Klopman, G. Chemical reactivity and the concept of chargeand frontier-controlled reactions. *J. Am. Chem. Soc.* **1968**, 90, 223– 234. (b) Fleming, I. *Frontier Orbitals and Organic Chemical Reactions*; Wiley, Chichester, UK, 2006; p 27.